UNCLASSIFIED

AD NUMBER

AD802424

NEW LIMITATION CHANGE

TO

Approved for public release, distribution unlimited

FROM

Distribution authorized to U.S. Gov't. agencies and private individuals or enterprises eligible to obtain export-controlled technical data in accordance with DoDD 5230.25 AUG 1966. Controlling DoD office is Space Systems Division, Los Angeles AFB, CA 90009-2960.

AUTHORITY

Aerospace Corp. ltr dtd 6 Apr 1967 per SSD/SSTP

THIS PAGE IS UNCLASSIFIED

AIR FORCE REPORT NO.
SSD-TR-66-180

AEROSPACE REPORT NO.
TR-669(6230-33)-1

802424

Dynamic Performance of Low Thrust Cold Gas Reaction Jets in a Vacuum

AUGUST 1966

Prepared by H. GREER
Applied Mechanics Division
El Segundo Technical Operations
and D. J. GRIEP
Electronics Division
El Segundo Technical Operations

Laboratory Operations
AEROSPACE CORPORATION

Prepared for BALLISTIC SYSTEMS AND SPACE SYSTEMS DIVISIONS
AIR FORCE SYSTEMS COMMAND
LOS ANGELES AIR FORCE STATION
Los Angeles, California

Air Force Report No.
SSD-TR-66-180

Aerospace Report No.
TR-669(6220-33)-1

DYNAMIC PERFORMANCE OF LOW THRUST COLD GAS REACTION JETS IN A VACUUM

Prepared by

H. Greer
Applied Mechanics Division
El Segundo Technical Operations

and

D. J. Griep
Electronics Division
El Segundo Technical Operations

Laboratory Operations
AEROSPACE CORPORATION
El Segundo, California

August 1966

Prepared for

BALLISTIC SYSTEMS AND SPACE SYSTEMS DIVISIONS
AIR FORCE SYSTEMS COMMAND
LOS ANGELES AIR FORCE STATION
Los Angeles, California

Best
Available
Copy

FOREWORD

This report is published by the Aerospace Corporation, El Segundo, California, under Air Force Contract No. AF 04(695)-669 and documents research carried out from March 1965 through April 1966. On 27 September 1966 this report was submitted to Capt. John T. Allton, STD, for review and approval.

The authors wish to acknowledge the contribution of Mr. Ford Cox, Equipment Analysis Section, who was instrumental in developing and operating the experimental apparatus.

Information in this report is embargoed under the U. S. Export Control Act of 1949, administered by the Department of Commerce. This report may be released by departments or agencies of the U. S. Government to departments or agencies of foreign governments with which the United States has defense treaty commitments. Private individuals or firms must comply with Department of Commerce export control regulations.

Approved

W. F. Radcliffe, Director
Engineering Sciences Subdivision
Applied Mechanics Division

for E. Levin, Director
Guidance and Control Subdivision
Electronics Division

for D. D. King, Director
Electronics Research Laboratory
Laboratories Division

Publication of this report does not constitute Air Force approval of the report's findings or conclusions. It is published only for the exchange and stimulation of ideas.

Approved

John T. Allton
Capt, USAF
Space Technology Division

ABSTRACT

The pulsed propulsive performance of low-thrust reaction jets, typical of those used for small spacecraft attitude control, is analyzed and compared with the results of laboratory experiments. Five gases, hydrogen, nitrogen, ammonia, Freon-12, and Freon-14, are investigated using a 48 to 1 expansion ratio nozzle. The transient processes which dominate the short-pulse or limit-cycle mode of thruster operation are formulated. These relationships show good correlation with the data. The apparatus, procedures, and techniques required to obtain accurate test results for a low-thrust, dynamic mode of operation are described. Impulse bit size, gas consumption, and specific impulse are characterized in terms of thruster geometry, gas properties, and command pulse width to provide a basis for optimum system design. A simplified method for calculating dynamic impulse bit size, dynamic gas consumption, and pulsed specific impulse as a function of command pulse width is developed. Finally, the effective performance of the gases tested is evaluated by a technique which includes the influence of tank and propellant weights, as well as specific impulse.

CONTENTS

ABSTRACT iii

NOMENCLATURE vii

I. INTRODUCTION 1

II. ANALYTICAL APPROACH 3

A. Pressure Transients 3

B. System Characteristics 11

C. Performance Losses 16

D. Transient Performance Approximations 25

E. Performance Comparison 27

III. EXPERIMENTAL PROGRAM 29

IV. CONCLUSIONS 39

REFERENCES 41

TABLE

1. Comparison of Performance Characteristics 17

FIGURES

1. Schematic of Experimental Apparatus 2
2. Typical Pulse Pressure History 4
3. Generalized Chamber Pressure Rise 8
4. Chamber Pressure Decay Transients 9
5. Dynamic Impulse Bit Correlation 12
6. Dynamic Gas Consumption Correlation 13
7. Pulsed Specific Impulse Correlation 15
8. Ammonia Expansion 20
9. Reaction Jet Cycle with Freon-12 21
10. Ammonia Condensate Impingement Pattern 23
11. Thrust Stand Assembly 30
12. Undamped Oscillation of Thrust Stand 32
13. Transient Response of Thrust Stand 32
14. Correlation of Thrust and Chamber Pressure for Hydrogen 33
15. Schematic of Command and Computer System 34
16. Total Impulse Distribution 36

NOMENCLATURE

A	=	area
a_1	=	$A_o a^* (2/\gamma)^{1/2} / 2V_c$
a_2	=	$(A_t a^* / 2V_c)[2/(\gamma + 1)]^{(\gamma+1)/2(\gamma-1)}$
a^*	=	acoustic velocity
B	=	equivalent orifice-to-nozzle area ratio
	=	$\frac{A_o}{A_t}\left(\frac{2}{\gamma}\right)^{1/2}\left(\frac{\gamma+1}{2}\right)^{\frac{\gamma+1}{2(\gamma-1)}} = \frac{a_1}{a_2}$
C_d	=	nozzle discharge coefficient
C_f	=	thrust coefficient
C_t	=	thrust correlation factor
C_v	=	exhaust velocity coefficient
D	=	diameter
F	=	thrust level
g	=	proportionality constant in Newton's second law
I	=	specific impulse
I_{eff}	=	effective system specific impulse
I_{tot}	=	total impulse
k	=	polytropic exponent

NOMENCLATURE (continued)

K_d	=	empirical decay time integration factor
K_n	=	choked nozzle flow factor
K_r	=	empirical rise time integration factor
M	=	Mach number
m	=	molecular weight
N_k	=	Knudsen number
N_r	=	Reynolds number
P	=	pressure
R	=	universal gas constant
T	=	temperature
V	=	volume
v	=	specific volume
W	=	weight flow rate
w	=	weight
y	=	pressure ratio transformation = $\left[1 - (P_c/P_s)\right]^{1/2}$
y_o	=	$\left[1 - (P_a/P_s)\right]^{1/2}$
γ	=	ratio of specific heats
ϵ	=	nozzle expansion ratio
η	=	efficiency

NOMENCLATURE (continued)

θ	=	time
ρ	=	density
σ	=	standard deviation = 0.7631×10^{-5} lb-sec or working stress
τ	=	dimensionless time factor = $a_2\theta$

SUBSCRIPTS

a	=	ambient
c	=	chamber or command
d	=	decay
e	=	nozzle exit
f	=	final
I	=	thermal
i	=	initial
n	=	nozzle
o	=	orifice
p	=	polytropic
r	=	reservoir or rise
s	=	steady state
t	=	throat

I. INTRODUCTION

The propulsive performance of various gases with a low expansion ratio (1.68 to 1) nozzle was reported in Refs. 1 - 3. In this document, propulsive performance and design relationships for cold gas jet reaction systems which might be used in small space vehicle attitude-control application are analytically derived and are correlated with the results of vacuum experiments using hydrogen, nitrogen, ammonia, Freon-12, and Freon-14 in a high expansion ratio (48 to 1) nozzle. These relationships, previously unavailable in systematic form, provide the analytical tools needed to design low thrust, pulsed, cold gas propulsion systems. A simplified means of calculating dynamic impulse bit size, gas consumption, and specific impulse is developed for use in preliminary design.

A schematic diagram of the experimental apparatus is shown in Fig. 1. Pressure and thrust histories and the weight of consumed gas were measured so that specific impulse could be determined as a function of command pulse width. A complete description of the experimental program is presented following a discussion of the analytical approach.

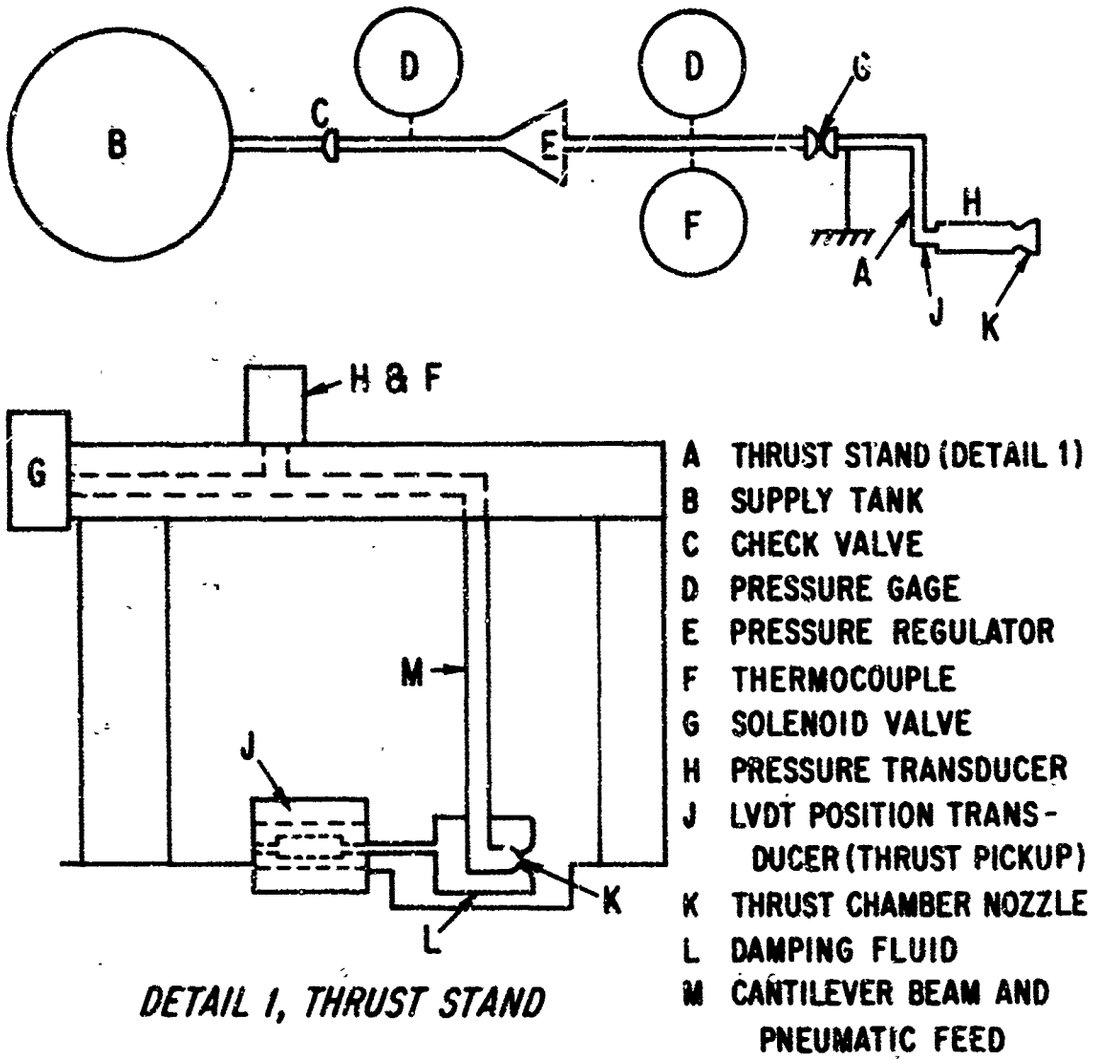

Fig. 1. Schematic of Experimental Apparatus

II. ANALYTICAL APPROACH

A. PRESSURE TRANSIENTS

The reaction jet performance is based on a dynamical analysis of the thrust chamber pressure history. In general, the chamber pressure history is composed of the steady-state and transient (startup and shutdown) phases illustrated in Fig. 2. In the following analysis, it is shown that the transient phase causes performance nonlinearities. Design relationships for predicting and optimizing these nonlinearities are developed.

During startup, the flow rate through the solenoid supply valve orifice W_o exceeds that through the discharge nozzle W_n, causing the chamber pressure P_c to build up. The exact expression for the compressible isentropic pressure buildup was given in Ref. 2 as

$$\frac{dP_c}{d\theta} = 2a_1 P_r \left(\frac{\gamma}{(\gamma - 1)}\right)^{1/2} \left[\left(\frac{P_c}{P_r}\right)^{2/\gamma} - \left(\frac{P_c}{P_r}\right)^{(\gamma+1)/\gamma}\right]^{1/2} - 2a_2 P_c \qquad (1)$$

For steady-state operation $dP_c/d\theta = 0$, and $P_c/P_r = P_s/P_r < 1$. This ratio is a design variable (typically on the order of 0.99) and is determined by the selection of A_o and A_t.

Equation (1) cannot be solved directly but may be simplified using one of three assumptions: (1) the thruster nozzle flow is zero during startup; (2) both nozzles are always choked; (3) the flow through the orifice occurs at constant density. For the case where the thruster nozzle flow is assumed

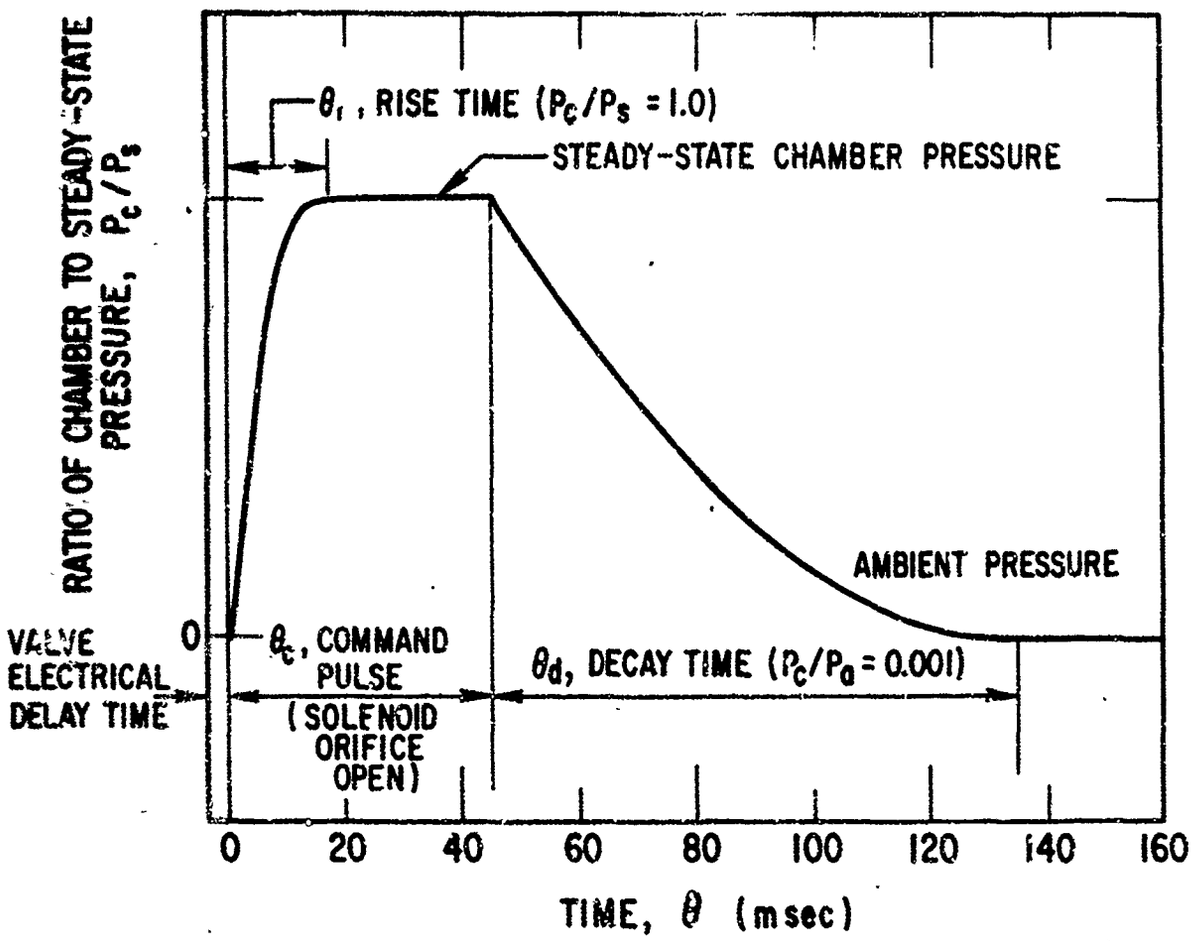

Fig. 2. Typical Pulse Pressure History

to be negligible during startup (assumption 1), Eq. (1) becomes

$$\frac{dP_c}{d\theta} = 2a_1 P_r \left(\frac{\gamma}{(\gamma - 1)}\right)^{1/2} \left[\left(\frac{P_c}{P_r}\right)^{2/\gamma} - \left(\frac{P_c}{P_r}\right)^{(\gamma+1)/\gamma}\right]^{1/2} \tag{2}$$

Integrating Eq. (2) between the appropriate limits results in

$$P_c/P_s = \left[1 - \left\{\left[1 - \left(1 - y_o^2\right)^{(\gamma-1)/\gamma}\right]^{1/2} - \left[(\gamma - 1)/\gamma\right]^{1/2} B\tau\right\}^2\right]^{\gamma/(\gamma-1)} \tag{3}$$

If both nozzles are assumed always choked (assumption 2), then Eq. (1) becomes

$$dP_c/d\theta = 2a_2(A_o P_r/A_t - P_c) \tag{4}$$

which integrates to

$$P_c/P_s = A_o/A_t + \left[1 - y_o^2 - (A_o/A_t)\right]e^{-2\tau} \tag{5}$$

Assuming constant density orifice flow (assumption 3), Eq. (1) becomes

$$dP_c/d\theta = 2a_1 P_r \left[1 - (P_c/P_r)\right]^{1/2} - 2\,a_2 P_c \tag{6}$$

Equation (6) can be integrated directly to obtain

$$-2\tau = \ln(-y^2 - By + 1) + \frac{2B}{(B^2 + 4)^{1/2}} \ln \frac{-2y - B - (B^2 + 4)^{1/2}}{(-y^2 - By + 1)^{1/2}} \Bigg|_{y_o}^{y^*} \quad (7)$$

To solve Eq. (7) explicitly for P_c/P_s, it is assumed** that B^2 is > 4, so

$$P_c/P_s = 1 - (y_o + B)^2 e^{-2\tau} + 2B(y_o + B)e^{-\tau} - B^2 \quad (8)$$

A comparison of the results obtained with Eqs. (3), (5), and (8) and measured data indicated better correlation over a wider range of variables when using Eq. (8). In addition, Eq. (3) is somewhat unwieldy to use, and Eq. (5) is valid only for $A_o/A_t > 1$ (or $B > 2$).

---

*An approximate approach would have been to assume that

$$\left[1 - (P_c/P_r)\right]^{1/2} \approx \left[1 - (P_c/2P_r)\right]$$

so Eq. (6) integrates to

$$\frac{P_c}{P_s} = \frac{2B}{(B + 2)} \left\{ 1 - \left[1 - \frac{(B + 2)P_a}{2BP_r}\right] e^{-(B+2)\tau} \right\}$$

**As the equivalent orifice-to-nozzle area ratio $B \to 1$, the orifice area restricts the gas flow (like a throttling orifice) so P_c never reaches P_r. To avoid this condition, B is usually sized > 2.

In Fig. 3, nondimensional solutions of Eq. (8) are presented for $y_o = 0.86$ to 1.0, $B = 1.0$ to 10.0, and $\tau = 0.005$ to 1.0. Good correlation between the analysis and the data for five gases (both at sea level and in vacuum) is noted. These results indicate that the time required to reach steady-state operation ($P_c/P_s = 1$) is significantly reduced by designing the jet reaction chamber with a small chamber volume (V_c) and a high ($B > 2$) orifice-to-nozzle area ratio.

From Eq. (8), the rise time, or the time required for the pressure in the thrust chamber to reach steady state ($P_c/P_s = 1$), is expressed by

$$\theta_r = (-B/a_1)\ln\left[B/(y_c + B)\right] \tag{9}$$

During shutdown, the orifice valve is closed and the gas accumulated in the chamber discharges through the nozzle. The instantaneous chamber pressure during an isentropic shutdown is given by

$$dP_c/d\theta = 2\gamma a_2 (P_{ci})^{(1-\gamma)/2\gamma} (P_c)^{(3\gamma-1)/2\gamma} \tag{10}$$

Integrating Eq. (10), the pressure ratio at time θ becomes

$$P_c/P_{ci} = \left[1 - a_2(1-\gamma)\theta\right]^{2\gamma/(1-\gamma)} \tag{11}$$

with the results as given in Fig. 4.

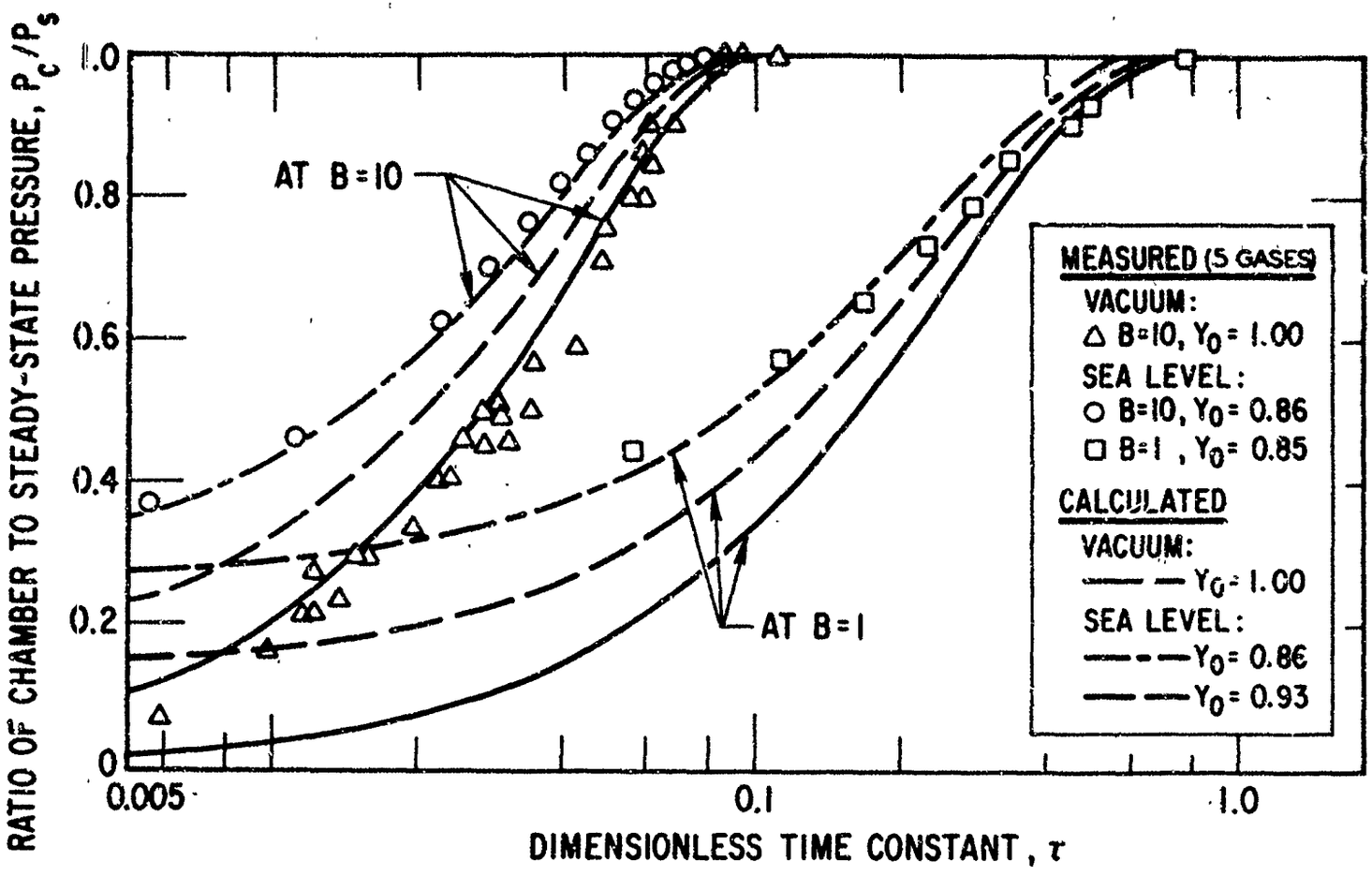

Fig. 3. Generalized Chamber Pressure Rise

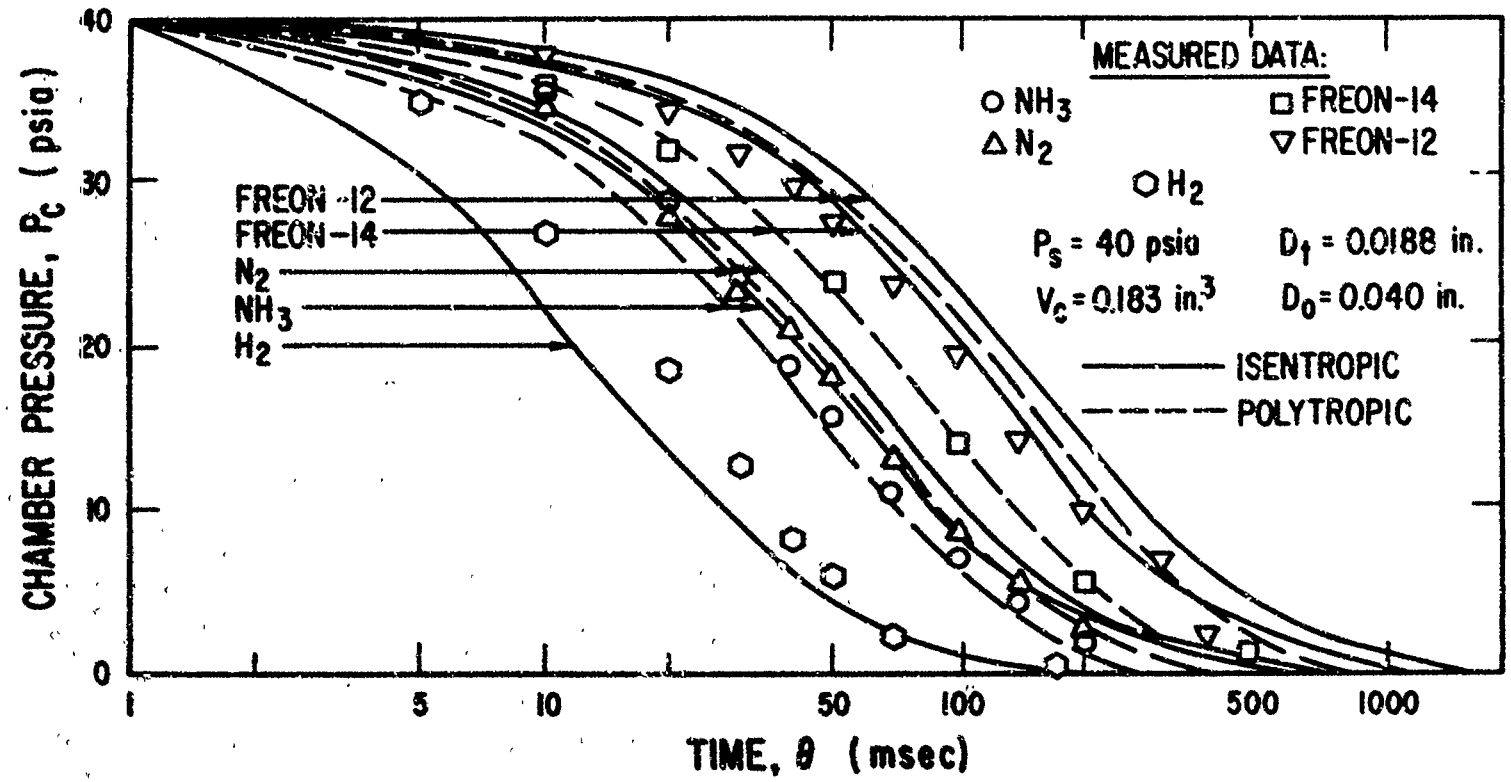

Fig. 4. Chamber Pressure Decay Transients

If the decay time θ_d is defined as the time required to discharge from P_s to P_a,*** then from Eq. (11)

$$\theta_d = [(P_a/P_s)^{(1-\gamma)/2\gamma} - 1]/a_2(\gamma - 1) \tag{12}$$

It can be seen that θ_d is a function of the gas properties and of V_c/A_t (chamber characteristic length).

The correlation between the ideal isentropic decay and the experimental results is not quite as good for the "slow" (low sonic speed) gases, such as the Freons, as for the "fast" gases, e.g., H_2 or NH_3. These fast gases discharge so rapidly that the time in which heat transfer and other non-isentropic imperfect gas effects can occur is restricted. The behavior of the more complex, heavy Freon molecules indicates that the decay transient for these gases follows a polytropic process.

In a polytropic expansion, deviations from isentropic perfect gas behavior are accounted for by adjusting the ratio of specific heats γ through a polytropic efficiency η_p to obtain a polytropic exponent k. This relationship between k and γ in terms of η_p is given by

$$k = \gamma/[\gamma + \eta_p(1 - \gamma)] \tag{13}$$

***In a vacuum, P_a/P_s was assumed equal to 10^{-3}.

The thermal expansion efficiency η_I is the square root of actual drop in gas temperature to the ideal temperature change and is related to polytropic efficiency by

$$\eta_I = \left[\frac{\left\{ (P_f/P_i)^{[(\gamma-1)/\gamma]\eta_p} - 1 \right\}}{(P_f/P_i)^{(\gamma-1)/\gamma} - 1} \right]^{1/2} \tag{14}$$

Values of η_p were determined from the test results, and the corresponding values of k and η_I were calculated. The results are listed in Table 1 for the gases tested (except H_2 which is so fast that its decay is well described by an isentropic decay). Better correlation is obtained by use of the polytropic exponents in the decay transient, as shown in Fig. 4.

B. SYSTEM CHARACTERISTICS

The thrust and nozzle flow transients are readily determined from the chamber pressure history. The dynamic impulse bit size (total impulse per pulse) and the dynamic gas consumption (gas consumed per pulse) are obtained by integrating the rise transient, the steady-state value (if $\theta_c > \theta_r$), and the decay transient of thrust and of gas flow. The thrust correlation factors and nozzle discharge coefficients listed in Table 1 (and discussed under Performance Losses) were used in the transient analysis to calculate impulse bit size and gas consumption, as functions of command pulse θ_c (defined as the time the valve is open) for the five gases shown in Figs. 5 and 6. Referring to Fig. 5, the difference between the theoretical and the measured values is due to the assumption of an isentropic decay. It was found (Ref. 3) that the correlation is improved if a polytropic expansion

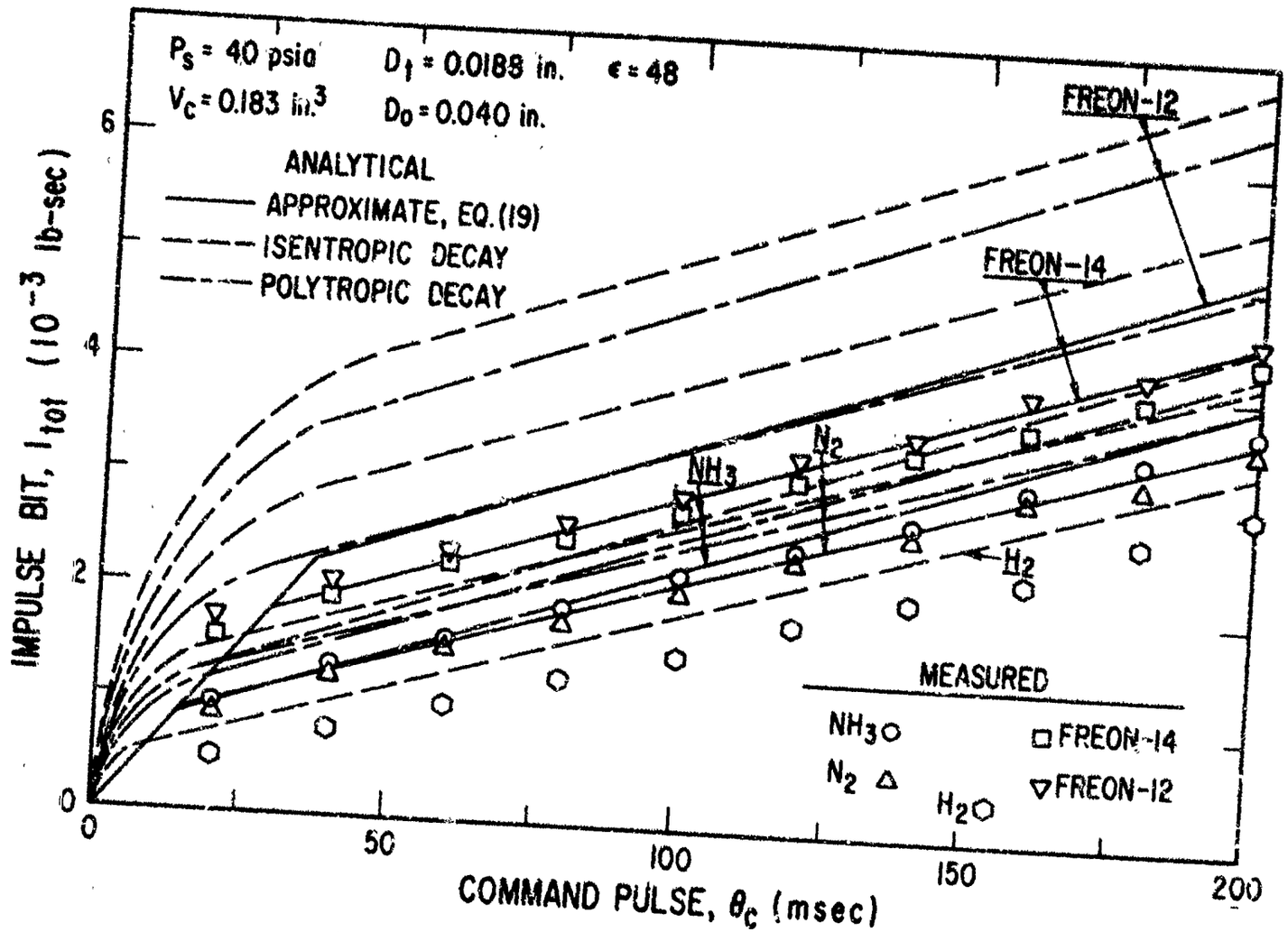

Fig. 5. Dynamic Impulse Bit Correlation

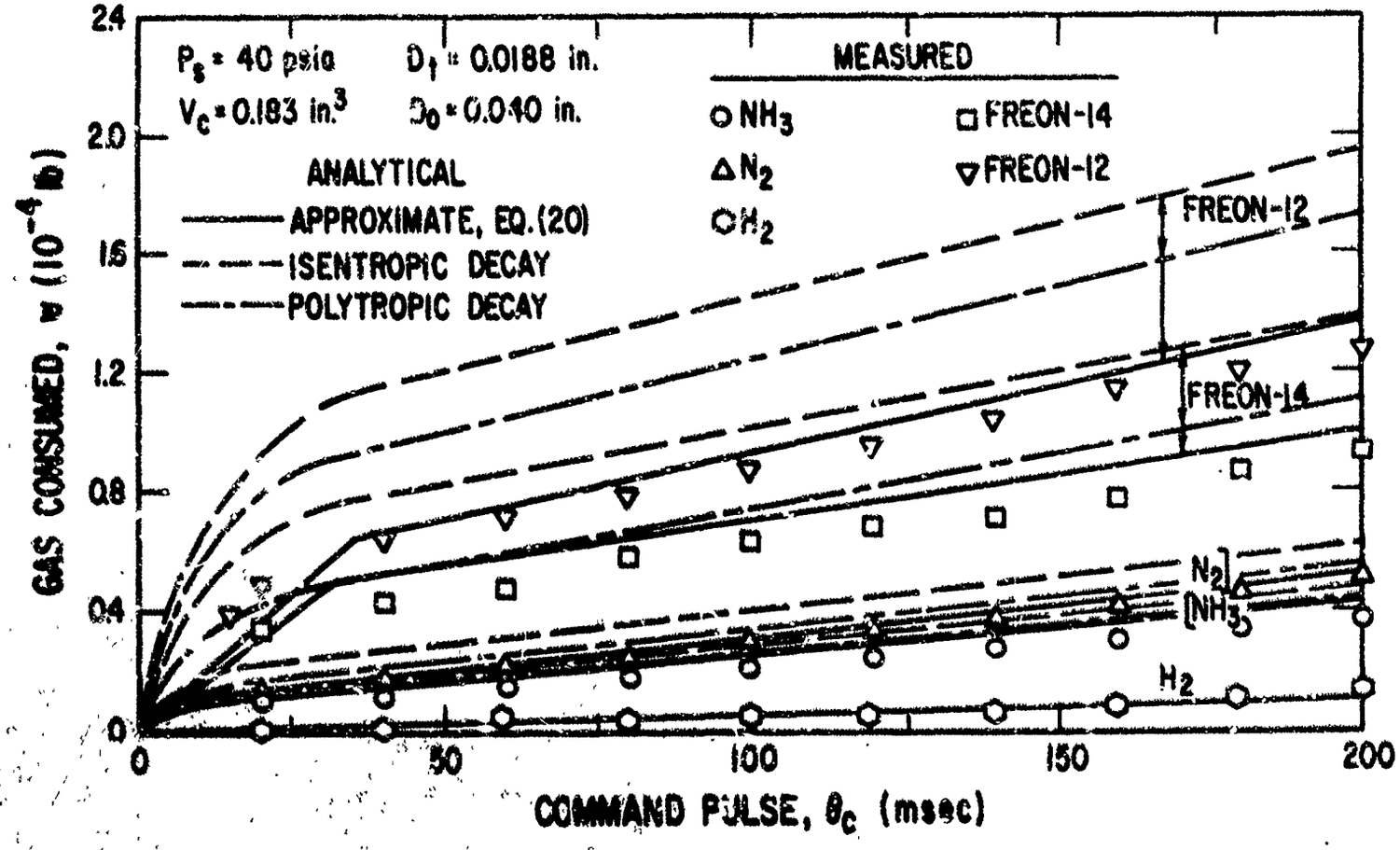

Fig. 6. Dynamic Gas Consumption Correlation

efficiency of about 85% is assumed when calculating impulse bit size and amount of gas consumed. However, specific impulse is not affected by the assumption of isentropic decay, and the polytropic approach is unnecessary for this calculation. Note that in the region of small command pulses ($\theta_c < \theta_r$), both impulse and consumption are nonlinear functions of command pulse. This nonlinearity, or deviation from the ideal square pulse-wave (instantaneous rise and decay), is produced by the rise and decay transients

Equations (8) and (11) provide the designer with relationships between the variables so that design tradeoffs may be evaluated. For minimum gas consumption at any given command pulse, the transients should be minimized or possibly designed to effectively complement each other; i.e., the ideal square pulse wave is approached if the integral of the chamber pressure over the decay time can be designed to compensate effectively for the initial difference between the product of the steady-state chamber pressure and the rise time and the integral of the chamber pressure over the rise time, i.e., $\int_0^{\theta_d} P_c d\theta$ should approach $P_s \theta_r - \int_0^{\theta_r} P_c d\theta$ for an ideal square pulse wave.

The dynamic (pulsed) specific impulse for five gases as a function of θ_c (Fig. 7) was obtained by dividing the impulse bit by the weight of gas consumed. For vacuum operation, specific impulse is essentially independent of command pulse duration† (unlike I_{tot} and w) and is close to the steady-state value. Figure 7 indicates good correlation between the analytical and experimental data.

†For command pulses less than 20 msec, the data becomes nonrepeatable because of valve dynamic limitations and increased experimental error.

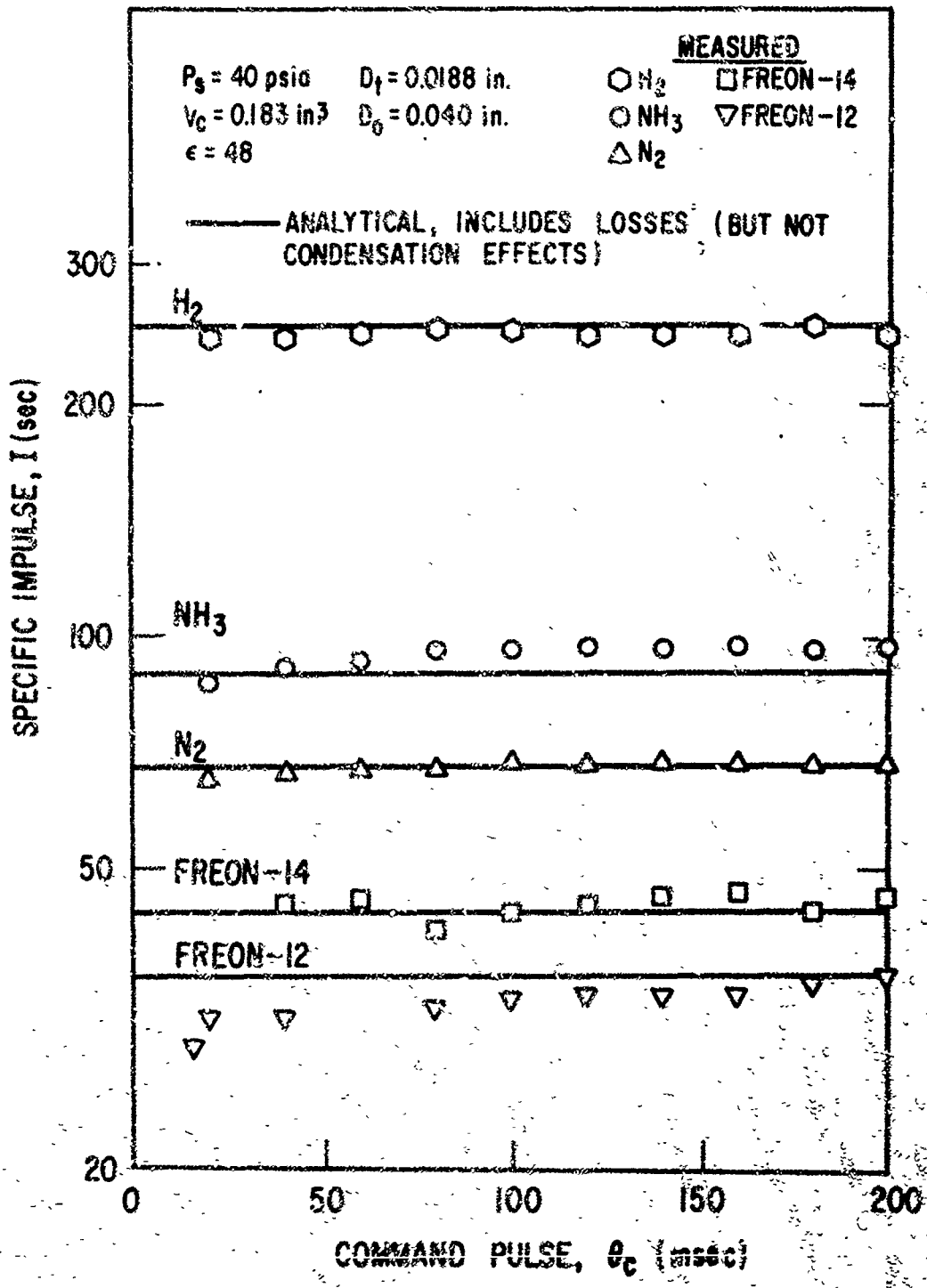

Fig. 7. Pulsed Specific Impulse Correlation

C. PERFORMANCE LOSSES

The tests in this study were made using a 15-degree half-angle conical aluminum nozzle with a measured throat diameter D_t of 0.0188 in. and an expansion ratio of 48 to 1. The steady-state chamber pressure was regulated to 40 psia; the gas temperature (downstream of the regulator) was 70°F. The ambient pressure in the vacuum chamber ranged from 300 to 1000 μ, depending on the thruster duty cycle.

The perfect gas isentropic flow relationships were used to calculate the ideal performance (e.g., characteristic velocity, nozzle exit pressure, and temperature) listed in Table 1. The tabulated ideal specific impulse does not include the effects of nozzle divergence and of the vacuum chamber pressure. Also listed in Table 1 are the nozzle throat Reynolds number (N_{rt} from 10,000 to 53,000), the nozzle exit Reynolds number (N_{re} from 3,000 to 18,000), and the nozzle exit Knudsen number (N_{ke} from 0.4×10^{-3} to 3.3×10^{-3}). Note that all of the gases operate in the coninuum flow regime ($N_k < 10^{-2}$) and that boundary layer viscous effects are not particularly severe ($N_{rt} > 10^4$). These effects may become important, however, for operation with values of N_k and N_{rt} considerably beyond the limits indicated.

The nozzle performance may be characterized by the discharge coefficient C_d (the ratio of actual weight flow to ideal isentropic weight flow) and the exhaust velocity coefficient C_v (the ratio of the average effective exhaust velocity to the ideal isentropic exhaust velocity). The ratio of the actual thrust coefficient to the ideal thrust coefficient defines the thrust

Table 1. Comparison of Performance Characteristics

Performance Characteristics	H_2	NH_3	N_2	Freon-14	Freon-12
Ratio of Specific Heats, γ	1.40	1.31	1.40	1.22	1.14
Molecular Weight of Gas, m	2	17	28	88	121
Characteristic Velocity, c* (fps)[a]	5260	1840	1400	835	720
Measured Steady-State Thrust, F_s (lb)	0.0146	0.0169	0.0147	0.0163	0.0176
Measured Steady-State Weight Flow, W_s (10^{-4} lb/sec)	0.55	1.87	2.17	3.69	4.84
Ideal Specific Impulse, I (sec)[a]	283	101	75	49	44
Nozzle Exit Pressure (microns)[a]	1500	2150	1500	3100	4300
Nozzle Exit Temperature (°R)[a]	67	105	67	164	250
Reynolds Number at Nozzle Throat, N_{rt}	10,000	27,000	20,000	32,000	53,000
Reynolds Number at Nozzle Exit, N_{re}	6,000	18,000	3,000	8,500	14,000
Knudsen Number at Nozzle Exit, N_{ke}	0.0014	0.0004	0.0033	0.0008	0.0004
Effective Nozzle Expansion Ratio, ϵ eff.	42	45	40	44	44
Polytropic Efficiency, η_p (%)	-	87	95	70	90
Polytropic Exponent, k	-	1.26	1.37	1.14	1.12
Thermal Expansion Efficiency, η_I (%)	-	95	95	87	91
Thrust Correlation Factor, C_t (%)	76	86[b]	76	78	80[b]
Discharge Coefficient, C_d (%)	84	98[b]	86	87	99[b]
Impulse Efficiency, C_v (%)	91	88-95[b]	89	92	83[b]
Nozzle Residence Time (μsec)	3	6	10	17	19
Measured Specific Impulse (sec)	260	96	67	46	37
Estimated Experimental Accuracy (%)					
θ_c = 20 msec	6.41	5.25	5.76	5.51	4.92
θ_c = 200 msec	5.34	4.83	5.32	5.31	4.82
Effective System Specific Impulse, I_{eff} (sec)	13	75[c]	28	32	29[c]

[a]Isentropic perfect gas expansion.

[b]Condensate may be present.

[c]Stored as a liquid, all others stored as gases at 3500 psia with $(\rho/\sigma)_t = 3.25 \times 10^{-5}$ ft^{-1} in Eq. (22).

correlation factor C_t, or

$$C_t = C_f/C_f \text{ ideal} = C_v C_d \tag{15}$$

It follows that C_v is equal to the impulse efficiency, or

$$C_v = C_t/C_d = I/I_{ideal} \tag{16}$$

The values of C_t and C_d in Table 1 are based on thrust and flow measurements taken in the Aerospace Guidance and Control Laboratory. The discharge coefficient of the test nozzle averaged about 0.85 for all the gases except NH_3 and Freon-12. The relatively high C_d of nearly 1.00 for these two gases was attributed to the presence of fluid condensate in the nozzle flow. The thrust correlation factor was also slightly higher for the condensable NH_3 and Freon-12 gases. The average impulse efficiency (C_v) was about 91%.[††] The efficiency of Freon-12 is slightly lower than average. This is attributed to: heavy molecular weight, uncertainties in thermodynamic properties, and very long transients. Values of C_v for NH_3 ranged from 88 to 95%, depending on the amount of condensation.

A method of correlating the losses associated with small nozzles in terms of throat Reynolds number and nozzle expansion ratio (Ref. 6) was

---

[††]This is also the average quoted in Refs. 4 and 5.

investigated.[9] No correlation could be obtained using the present data (a similar lack of correlation of C_f and C_v in terms of Reynolds number was reported in Ref. 7). The results indicate that the difference between the ideal isentropic thrust coefficient and the measured thrust coefficient is a constant of about 0.39 (except for NH_3) and is independent of the throat Reynolds number.

In addition, an analysis of the boundary layer (Ref. 8) was made to determine its effect on nozzle performance. The effective nozzle expansion ratios were found to be up to 20% less than the geometric ratios (see Table 1) with a consequent performance loss of about 3%. It was estimated that viscous losses and changes in the free-stream flow conditions introduced by the boundary layer would result in about 3% additional losses. The total losses, including divergence and vacuum backpressure (but not condensation), are estimated to be about 9%.

Isentropic reaction jet expansions of NH_3 and Freon - 12 are shown on Mollier diagrams in Figs. 8 and 9. The ideal expansion end-point of either gas is well into the two-phase (liquid-vapor) mixture region so that a metastable supersaturated condition would be expected to occur in the nozzle. The NH_3 expansion not only crosses the saturation line but also crosses the triple line (solid-liquid-vapor) into a solid-vapor region. Since incipient condensation of steam is known to occur at the 5%

[9] The data in Ref. 6 was obtained for only one gas, H_2, and at Reynolds numbers generally less than 10,000, whereas the values of N_{rt} for the five gases tested in the present investigation ranged from 10,000 to 53,000.

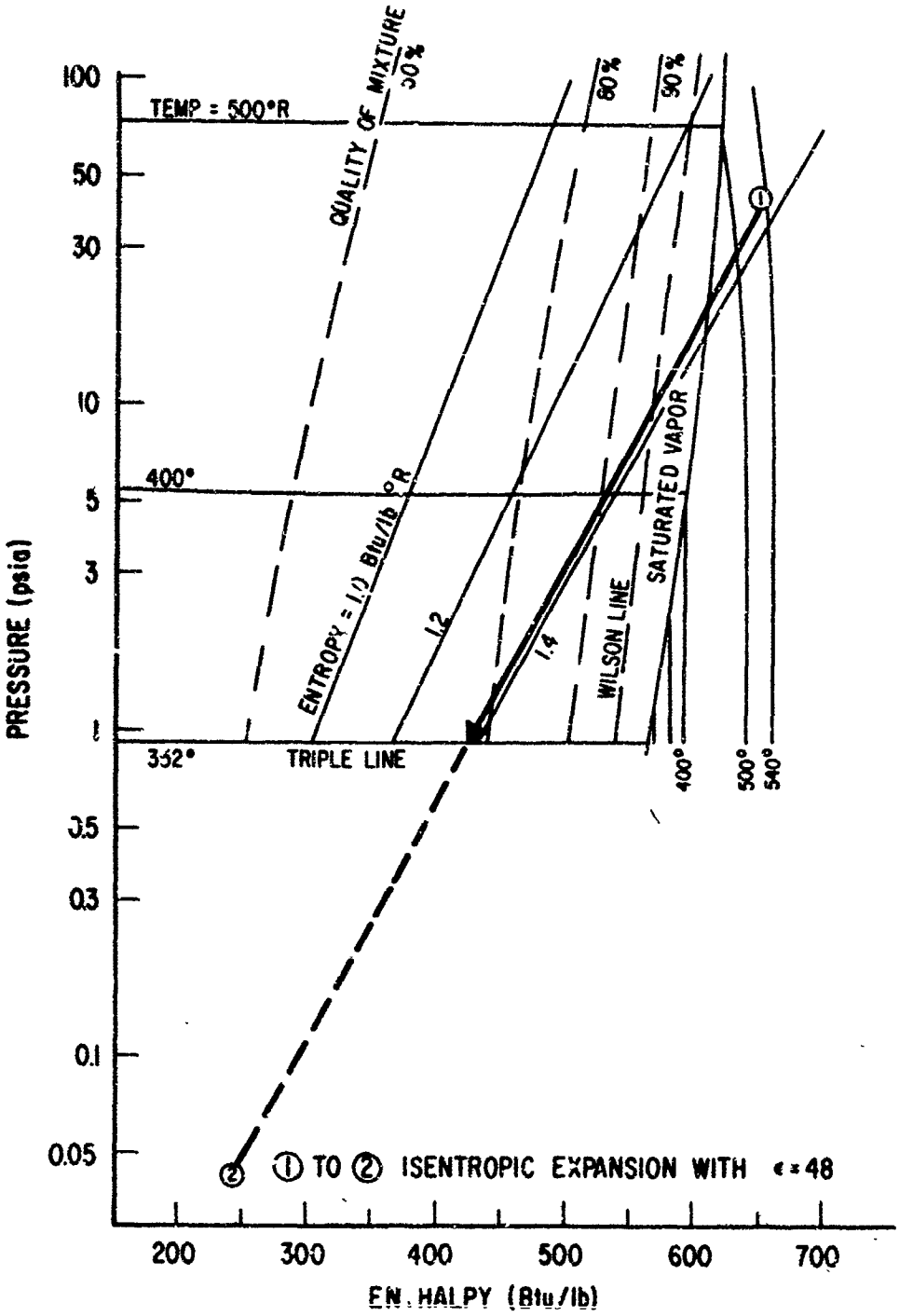

Fig. 8. Ammonia Expansion

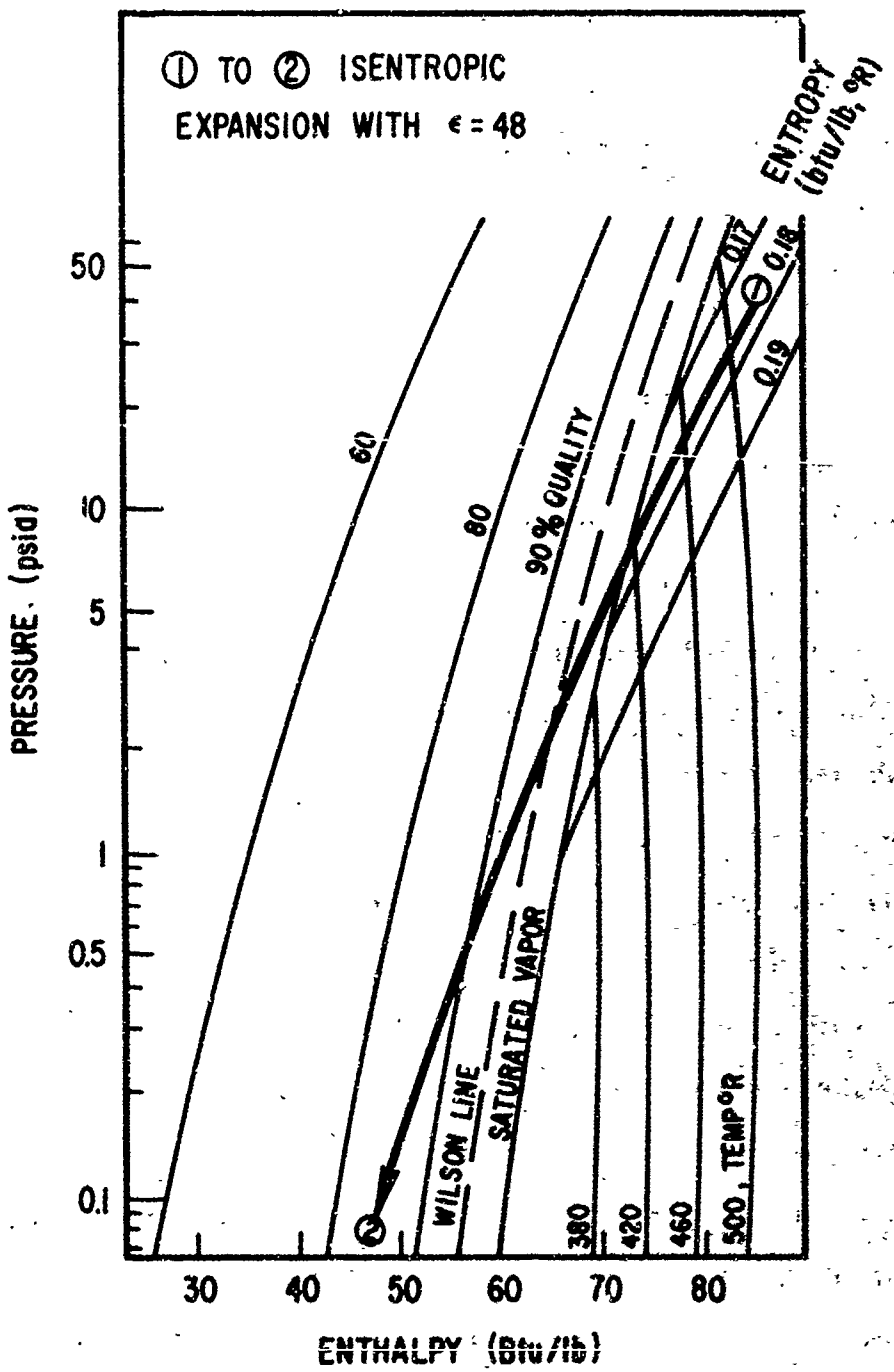

Fig. 9. Reaction Jet Cycle with Freon-12

liquid or Wilson line (Ref. 9), it is reasonable to assume that highly super-saturated conditions in the test gases cannot be sustained without condensation occurring, thus resulting in significant deviation from an ideal constant-entropy expansion process.

The problem of small nozzle condensation was first observed in the present study when NH_3 and Freon-12 were tested at sea level (Ref. 1). The existence of liquid condensate in the nozzle discharge was demonstrated experimentally (Ref. 3) through hot-wire conductivity measurements and by photographing the fluid impingement pattern produced on a black matte target downstream of the nozzle (Fig. 10). Attempts at direct observation of the condensate droplets in a transparent nozzle through the Tyndall effect (backscattering of a light beam) were inconclusive, probably because the droplets in the nozzle were smaller than the wavelength of the light and were moving at a high velocity (short residence time). The small size of the nozzle also hampered direct optical viewing of the condensate.

The present theoretical treatment of nucleation and droplet growth during condensation from vapor (i.e., the disappearance of vapor molecules and the formation and growth of fluid droplets) appears unable to produce definitive quantitative results. One major difficulty concerns nucleation kinetics or the reactions (and rates) by which vapor molecules combine to form droplets (Refs. 10 - 16). The treatment of the influence of foreign impurities, e.g., dust or ions, which provide heterogeneous nuclei and promote condensation, presents additional difficulties. In the present study, the pulsed or dynamic mode of operation introduces another transient consideration. Even for steady-state operation, the small nozzle size and the

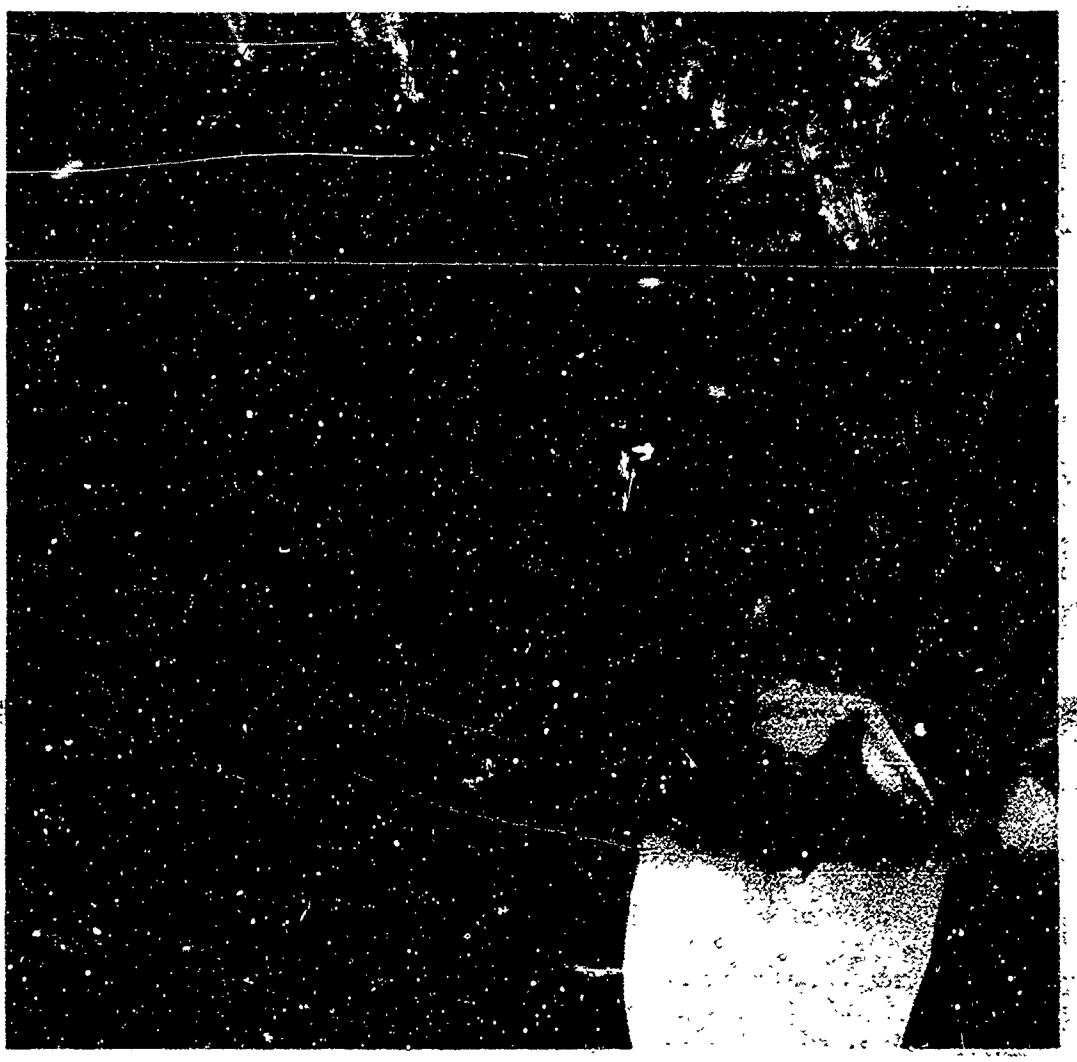

Fig. 10. Ammonia Condensate Impingement Pattern

short residence time (Ref. 15) involved (see Table 1) present theoretical problems concerning scale effects.

Although the problem of determining the effect of flow condensation on nozzle performance has been recognized for 40 years (Ref. 17), the experimental work in homogeneous nucleation and condensation is apparently meager, particularly with respect to pulsed flow in very small nozzles.* Most of the previous experimental work has been done using saturated water in large nozzles (Refs. 9, and 16 - 20) or in cloud chambers (Ref. 21). The qualitative indications are that the actual flow is somewhat greater than would be theoretically expected. In the present study, the observed increase in C_d for the NH_3 and Freon-12 was attributed to the presence of fluid condensate.

Theoretical methods (Refs. 22 and 23) for calculating the condensation losses were examined. These results indicate from 3 to 7% additional performance loss for two-phase expansion due to: energy transfer between vapor and droplets (a part of which is lost by dispersion); the appearance of supercooled states and impact (shock) condensation; and (possibly) lack of time for interphase thermal equilibrium.

In summary, because the effects of condensing vapors on small nozzle expansion processes are presently not well understood, additional

*Accurate measurements are usually difficult to obtain with small nozzles (D_t < 100 mils), e.g., measurement of A_t may be in error by 10%. Also, microscopic differences in construction could alter the nozzle flow characteristics.

study is required in order to establish accurate means of performance analysis and characterization.

D. TRANSIENT PERFORMANCE APPROXIMATIONS

When the rise and decay thrust and flow rate transients are integrated, it is possible to define time integration factors so that

$$K_r = \frac{\int_0^{\theta_r} P_c \, d\theta}{P_s \theta_r} \tag{17}$$

and

$$K_d = \frac{\int_0^{\theta_d} P_c \, d\theta}{P_s \theta_d} \tag{18}$$

Using these empirical factors, dynamic impulse bit size, dynamic gas consumption, and pulsed specific impulse can be obtained from the following approximate relationships.

Impulse Bit Size

For $\theta_c \leq \theta_r$,

$$I_{tot} = C_f A_t P_s (K_r \theta_r + K_d \theta_d)(\theta_c / \theta_r)$$

For $\theta_c \geq \theta_r$, (19)

$$I_{tot} = C_f A_t P_s \left[K_r \theta_r + (\theta_c - \theta_r) + K_d \theta_d \right]$$

Gas Consumption

For $\theta_c \leq \theta_r$,

$$w = K_n A_t P_s (K_r \theta_r + K_d \theta_d)(\theta_c / \theta_r)$$

For $\theta_c \geq \theta_r$,

$$w = K_n A_t P_s \left[K_r \theta_r + (\theta_c - \theta_r) + K_d \theta_d \right] \tag{20}$$

where

K_n = choked nozzle flow factor

$$= a^* \left[2/(\gamma + 1) \right]^{(\gamma+1)/2(\gamma-1)} / RT$$

For the gases tested in this study, values of $K_r = 0.69$ and $K_d = 0.0685$ were found to provide good correlation with the measured data.[□] Comparison of these approximate results with those obtained with the isentropic analysis, the polytropic analysis, and the data are shown in Figs. 5 - 7.

Specific Impulse

The specific impulse is the ratio of Eq. (19) to Eq. (20), or simply

$$I = \frac{\int C_f A_t P_c d\theta}{\int K_n A_t P_c d\theta} = \frac{C_f}{K_n} \tag{21}$$

[□] $K_d = 0.13$ was found to provide good correlation with an isentropic decay, whereas $K_d = 0.0685$ correlated with the polytropic decay process.

It is noted from Eq. (21) that specific impulse is theoretically constant and independent of command pulse θ_c.

E. PERFORMANCE COMPARISON

Although specific impulse is the most important single measure of propulsive performance, other factors become important for system design. As pointed out in Ref. 24, consideration should be given to the propellant density and associated tankage weight. This may be accomplished by defining effective system specific impulse as the ratio of delivered total impulse to the combined propellant and minimum spherical tankage weight. Thus

$$I_{eff} = I/\left[1 + 1.5vP(\rho/\sigma)_t\right] \tag{22}$$

where

P = the propellant storage pressure (typically 3500 psia)

v = the propellant specific volume

$(\rho/\sigma)_t$ = the ratio of tank density to working stress = 3.25×10^{-5} ft^{-1} for titanium with a safety factor of 2.

This technique was applied to the measured values of specific impulse for the five gases tested. The results are listed in Table 1. The condensable gases, NH_3 and Freon-12, were assumed stored as liquids at their room temperature vapor pressures of 130 and 85 psia, respectively, and Eq. (18) was modified to account for minimum gage tanks, based on actual spacecraft design. It is noted that on the basis of specific impulse, H_2 has the highest performance (260 sec), whereas on the basis of effective system specific impulse, H_2 has the lowest performance (13 sec). On the basis of effective system specific impulse, NH_3 has the highest performance (75 sec) and Freon-12 is competitive with N_2 at 28 sec. However, a weight penalty for the heat of

vaporization of NH_3 and Freon-12 was not included in the Table 1 performance values. (In the laboratory this heat was provided by the heat capacity of the apparatus.) In the case of NH_3, about 500 Btu/lb are required for vaporization. This heat would either have to be supplied from the heat capacity of the spacecraft or from an external source, depending on the application. The final selection of one propellant over another would depend on the results of a detailed design study for a specific mission.

III. EXPERIMENTAL PROGRAM

The experimental apparatus shown in Fig. 1 includes a regulated cold-gas pneumatic system, a thrust stand, and an electronic command and computer system.

The cold-gas pneumatic system consists of a pressure vessel for propellant storage, a 0 to 400 psi pressure gage, a thermocouple temperature monitor, a pressure regulator adjustable from 0 to 100 psi, and a low pressure monitor gage. When the system is operated on H_2, N_2, or Freon-14, pressure and temperature measurements are used to determine propellant mass consumption from the physical properties (Refs. 25-28). When the system is operated with anhydrous NH_3 or Freon-12, the storage vessel is accurately weighed before and after a test to determine the mass consumed during the test. A typical test consists of several thousand pre-programmed command pulses.

The thrust measurement apparatus, Fig. 11, has a nozzle mounted on the end of a short length of tubing to serve the dual function of a pneumatic feed line and a cantilever beam spring. When thrust is produced, the beam is displaced in an amount proportional to the thrust magnitude. The deflection of the beam is sensed by a position transducer, and an electrical output proportional to the position (thrust level) is generated. Critical viscous damping is provided through the shearing action of a flat plate moving through a viscous fluid. A high, natural frequency of the cantilever beam and nozzle assembly (250 cps) is necessary to provide adequate dynamic response for the thrust transients.

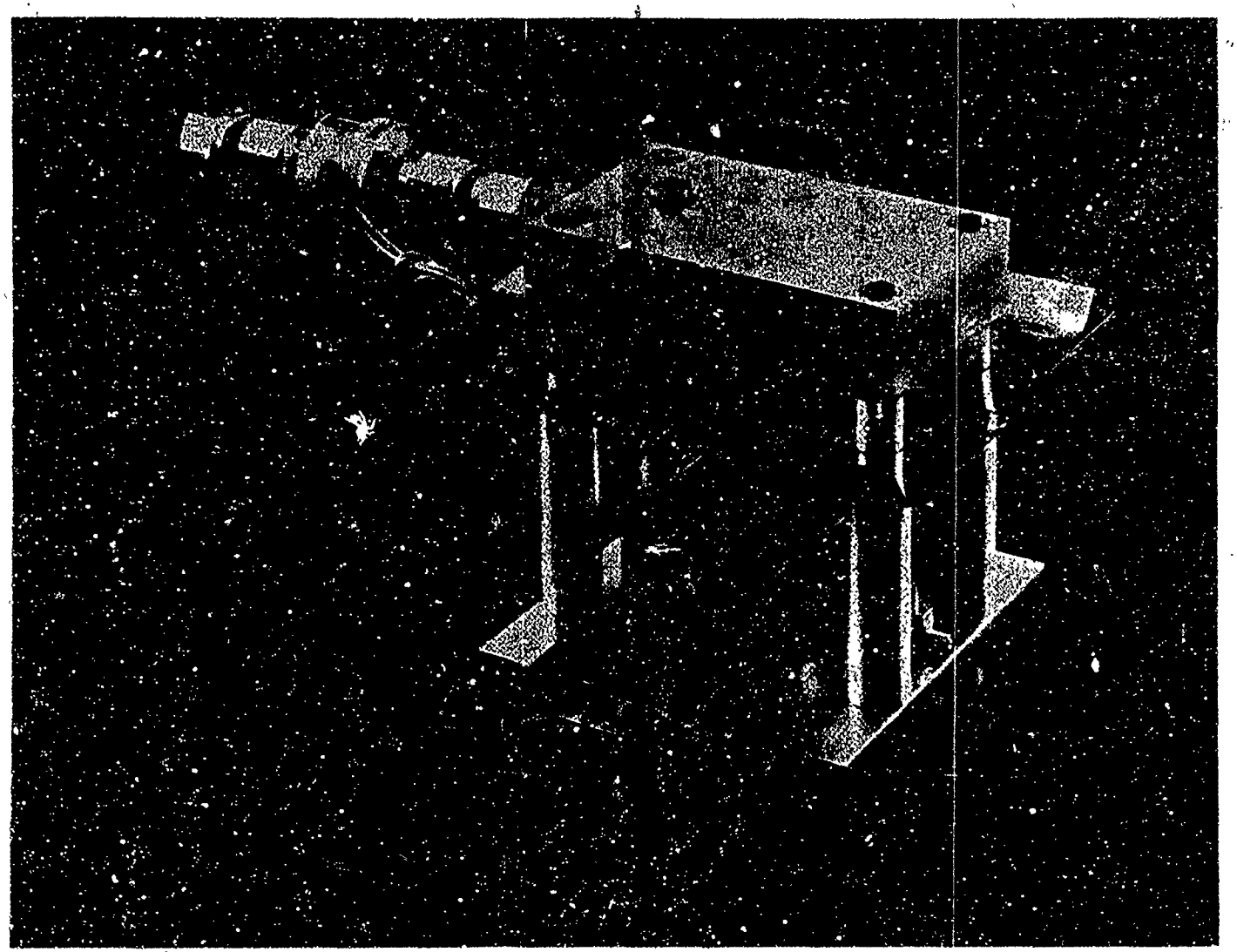

Fig. 11. Thrust Stand Assembly

The natural frequency of the thrust measurement fixture was verified experimentally by two methods. The first was displacement of the beam by a discharge of gas from the pneumatic system through the nozzle. The natural frequencies of the fixture, both with and without damping fluid, were displayed on the oscilloscope and photographed. A photograph of the undamped oscillation is shown in Fig. 12. The second method was positioning a coaxial solenoid valve in such a way that high pressure air would discharge through the valve and impinge on the thrust fixture nozzle block. The resulting displacement of the fixture was monitored on the oscilloscope. By adjusting the high pressure air supply valve, the peak cantilever beam displacement was set equal to the displacement experienced during thrust measurement. Figure 13 is a photograph of the transient response of the thrust stand excited by such an external force. The thrust stand dynamic response is more than adequate for the rise times encountered, as evidenced by the correlation of thrust and pressure traces in Fig. 14. (A pressure transducer with a 1200 cps acoustic frequency was used to monitor pressure.)

The thrust stand was calibrated in two ways: (1) using a Scherr-Tumico force gauge and providing a scale factor in terms of volts per pound of force; (2) orienting the thrust stand so that the beam was subjected to a 1 g loading. Test weights were then placed on the cantilever beam, and a correlation of force versus electrical output (deflection) was made. Both methods were in excellent agreement.

A schematic of the command and computer system is shown in Fig. 15. A preset counter or clock was used to fix the repetition rate of the command

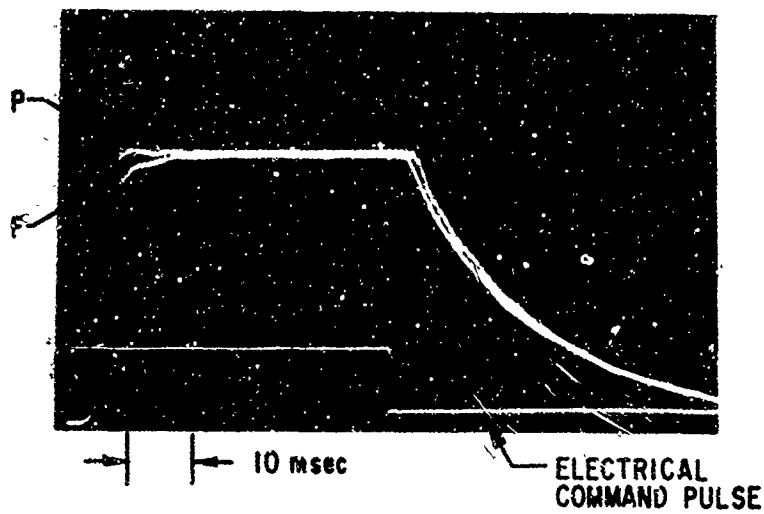

Fig. 14. Correlation of Thrust and Chamber Pressure for Hydrogen. (steady-state thrust = 0.0146 lb; steady-state chamber pressure = 40 psia; command pulse = 50 msec)

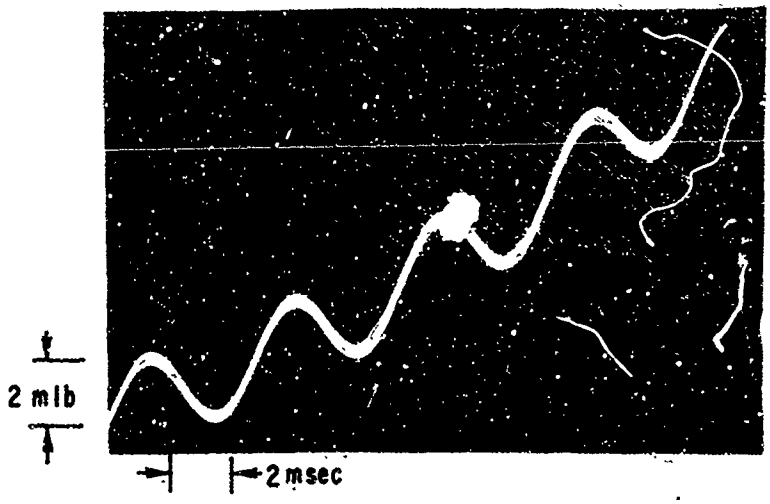

Fig. 12. Undamped Oscillation of Thrust Stand

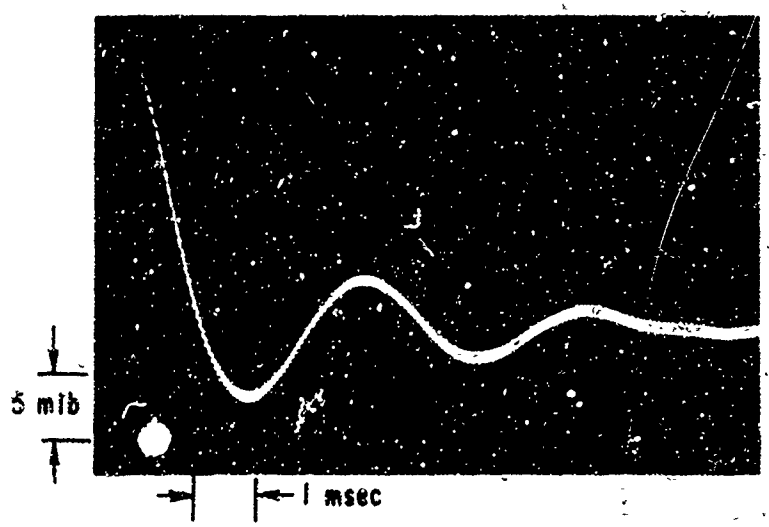

Fig. 13. Transient Response of Thrust Stand Using External Forcing Function Input.

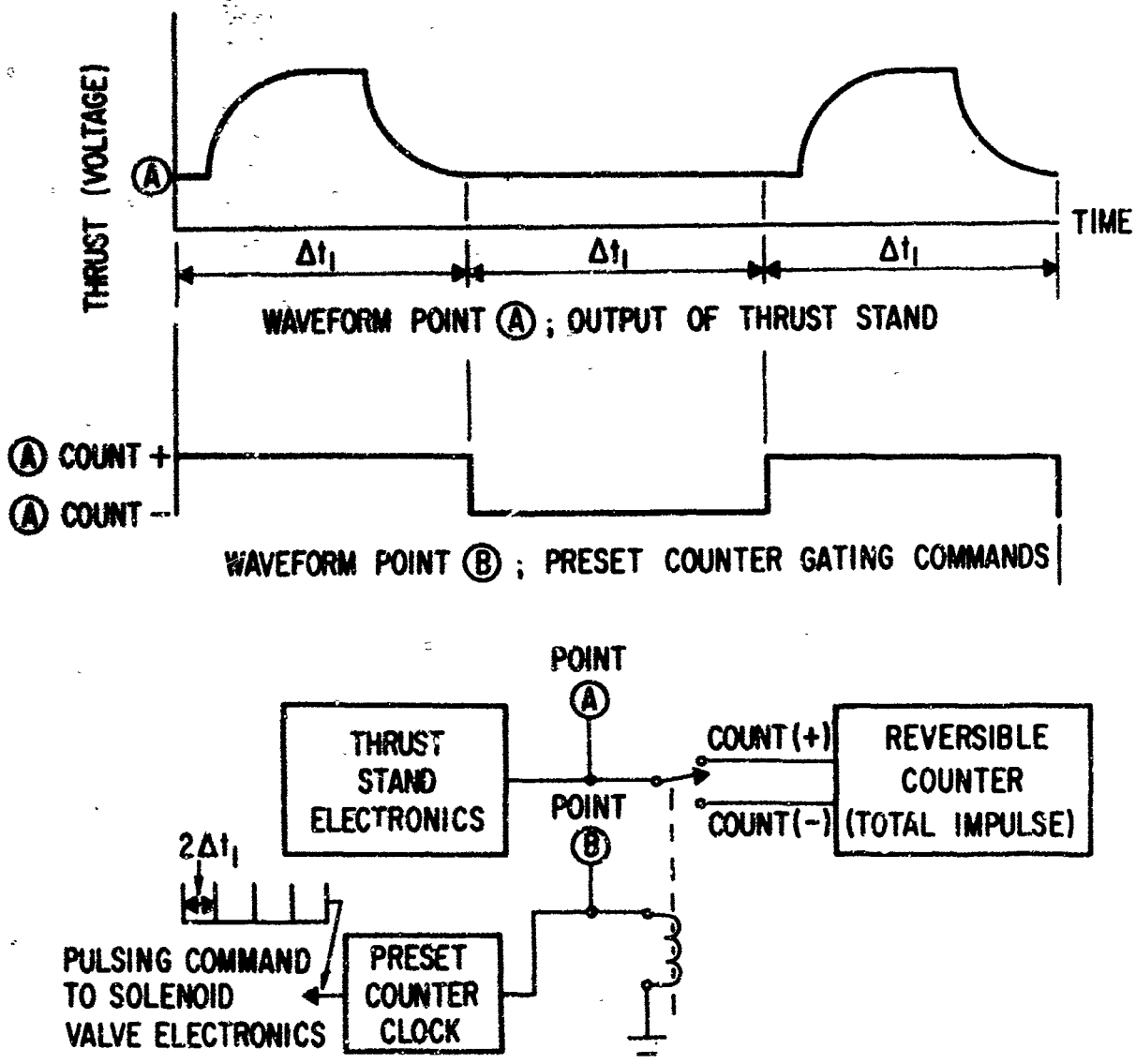

Fig. 15. Schematic of Command and Computer System

pulses, and a digital counter recorded the number of cycles or pulses applied to the solenoid valve. The output of the thrust transducer was amplified, demodulated, and fed to the voltage-to-frequency converter. The output of the converter was fed into a reversible counter which was used to integrate the thrust profile and thus obtain the total impulse per pulse (impulse bit size). The reversible counter computed the impulse bit including drift or offset during a time increment Δt. Then, the counter totalled the integrated offset and drift for an equal time increment Δt and obtained the difference between the two values to provide a direct readout of total impulse. The reversible counter provided improved accuracy over the two separate counters previously used (Ref. 3) for the same function by eliminating any errors due to differences in timing sensitivity between individual counters.

The specific impulse was obtained by dividing the total impulse by the gas consumed as measured over a large number of command pulses (>1000). The solenoid valve closing time was adjusted to equal the valve opening time by valve driver circuitry modifications (Ref. 29). Therefore, this configuration resulted in a valve open time equal to the electrical command pulse width, with a 3.5-msec delay relative to the command pulse.

To complete the experimental evaluation, the repeatability of impulse bit size was verified. Two thousand 20-msec command pulses were applied to the solenoid valve, and the total impulse of each pulse was recorded. The distribution plot of these data, Fig. 16, indicates the excellent repeatability of impulse bit size.

An estimated error analysis of the experimental configuration was made. This analysis included the effects of mass measurement errors, limited

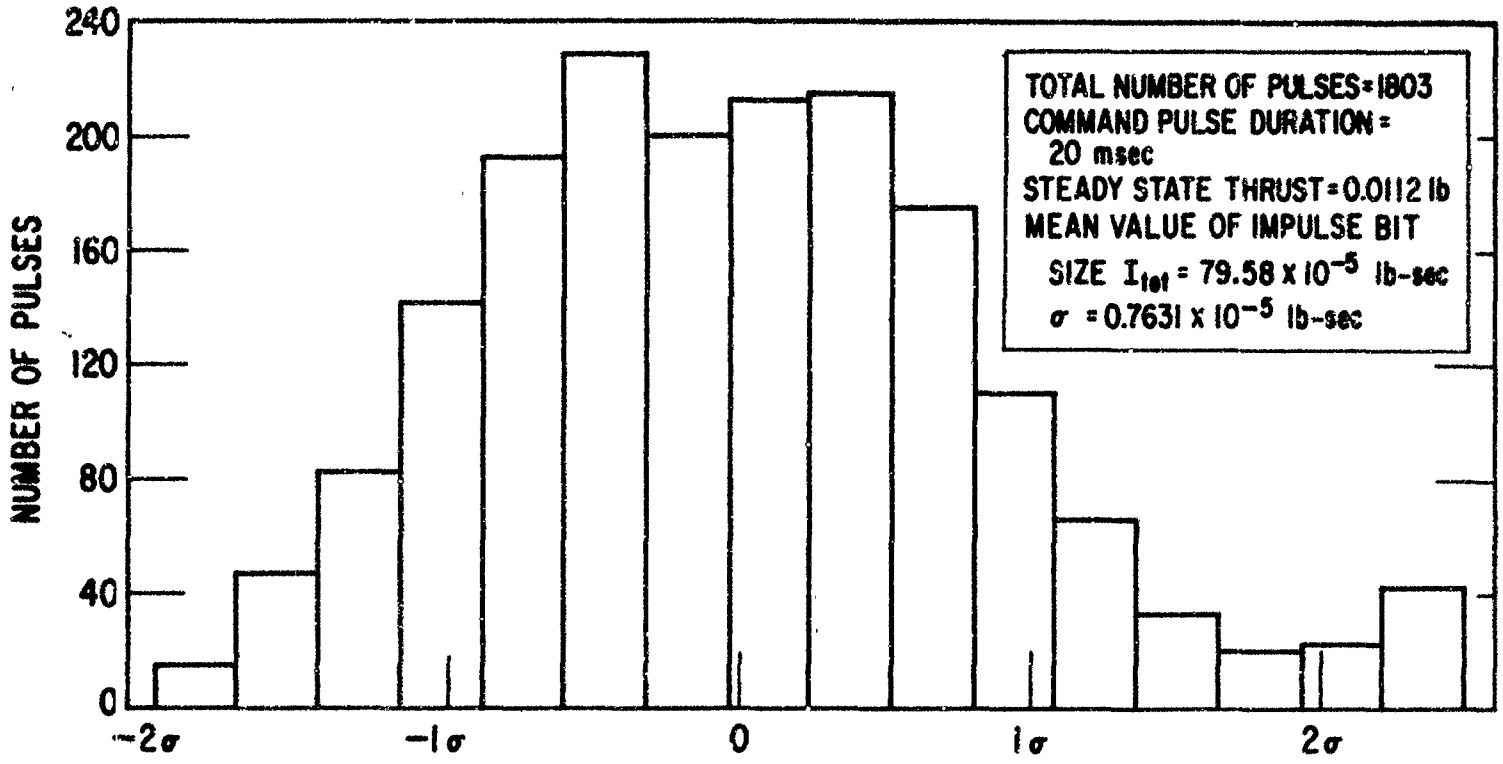

Fig. 16. Total Impulse Distribution

dynamic response of the thrust fixture, calibration errors, and electronic errors. The error estimate took into account the variation in experimental measurement accuracy with command pulse width and with the propellant used. The average error for all propellants and command pulse widths is approximately 5%, the typical spread of measured data points. Table 1 presents the estimated measurement error associated with each propellant for command pulse durations of 20 and 200 msec. The predicted measurement accuracy of 5% correlates well with the experimental data. In Fig. 7 for example, 80% of the experimentally measured data lies within 5% of the theoretical predictions.

During the course of the experiments, a leakage problem became apparent when testing H_2. Because of the low molecular weight of H_2 (see Table 1), a leak of only 1.25×10^{-6} lb of gas while obtaining a data point would produce a 20% error in measured specific impulse. The same quantity of leaking N_2 would result in a 5% error in specific impulse. It was found that the leak was caused by the O-ring used to seal the nozzle in the nozzle block and could have been prevented by careful installation.

An additional problem was encountered during the H_2 experiments. Significant variations in specific impulse were observed during the initial tests. Subsequent investigation revealed that these variations were due to the effects of gaseous contamination occurring during the filling of the propellant tank. Normally, when the propellants were changed (e.g., changing from N_2 to H_2), the complete pneumatic system was evacuated using a vacuum pump to remove residual gases. Then the propellant tank was filled

with the new gas. However, ambient air in the 4-ft long fill hose had not been considered. Calculations indicated that the error in specific impulse introduced by the contamination of H_2 with trapped air could be as large as 20% due to the change in the average gas molecular weight. This conclusion was experimentally verified. The propellant loading procedure was then modified to include a vacuum purge of the propellant fill line as well as of the pneumatic system.

IV. CONCLUSIONS

Accurate predictions of impulse bit size, gas consumption, and effective specific impulse can be made using the gas dynamical relationships given for the transient pressure histories. These relationships constitute an effective analytical tool for optimizing system performance for a given control requirement.

Both the gas consumed and the impulse bit size are nonlinear functions of command pulses for small pulses but become linear when steady-state chamber pressure is reached. The nonlinearity, or deviation from the ideal square pulse-wave, is due to the rise and decay transients. For minimum gas consumption at a given command pulse, the transients can be minimized by proper design so that the rise transient effects are essentially offset by the decay transient effects. A simplified approach to transient performance determination given by Eqs. (19) through (21) can be used for preliminary design purposes.

The pulsed vacuum specific impulse is essentially independent of command pulse width and is close to the steady-state value. A loss of from 5 to 10% in specific impulse was observed for command pulses less than 20 msec. This degradation is attributed to the increasing dominance of solenoid valve dynamics. Because of increasing interest in small pulse-width performance (<20 msec), additional study in this area is required in order to characterize solenoid valve dynamic effects on performance.

This discharge coefficient of the nozzle tested averaged about 85% for all the gases except NH_3 and Freon-12. The average impulse efficiency was about 91%. No correlation of the nozzle losses could be obtained in terms of Reynolds number. The results indicate a constant loss in ideal isentropic thrust coefficient of approximately 0.39 (except for condensing gases, NH_3 and Freon-12). Additional study is warranted on the subject of small nozzle expansion processes and on the performance effects of condensing vapors.

On the basis of specific impulse alone, H_2 shows the highest performance. If propellant and tank weights are considered, then NH_3 has the highest effective system specific impulse. Since the NH_3 was assumed to be stored as a liquid, the effect of the required heat of vaporization would have to be considered in spacecraft design applications. The final selection of propellant should be based on a detailed study of the specific mission requirements.

REFERENCES

1. Griep, D. J., "Experimental performance of anhydrous ammonia," Aerospace Corp. TDR-469(5230-33)-1 (12 October 1964).
2. Greer, H., "Analytical investigation of nitrogen jet reaction control systems," Aerospace Corp. TDR-469(5560-30)-1 (30 November 1964).
3. Greer, H. and Griep, D. J., "Low-thrust reaction jet performance," Aerospace Corp. TDR-469(5230-33)-2 (August 1965).
4. Sutton, G. P., Rocket Propulsion Elements (J. Wiley & Sons, Inc., New York, 1956), 2nd ed., p. 77.
5. Sutherland, G. S. and Maes, M. E., "A review of micro-rocket technology: 10^{-6} to 1-lb thrust," AIAA Paper No. 65-520 (14 June 1965).
6. Spisz, E. W., Brinck, P. F., and Jack, J. R., "Thrust coefficients of low-thrust nozzles," NASA Lewis Research Center, TN D-3056 (October 1965).
7. Tinling, B. E., "Measured steady-state performance of water vapor jets for use in space vehicle attitude control systems," NASA Ames Research Center, TN D-1302 (May 1962).
8. Schlichting, H., Boundary Layer Theory (Pergamon Press, New York, 1955), pp. 281-297.
9. Yellott, J. I. and Holland, C. K., "Condensation in diverging nozzles," Trans. ASME, Vol. FSP-59-5, 161-183 (1937).
10. Hischefelder, J. O., Curtiss, C. F., and Bird, R. B., Molecular Theory of Gases and Liquids (J. Wiley & Sons, Inc., New York, 1964), pp. 377-390, 405-407.

11. Frenkel, J., Kinetic Theory of Liquids (Dover Publications, Inc., New York, 1955), pp. 365-413.

12. Courtney, W. G., "Condensation in Nozzles," Ninth Symposium on Combustion (Academic Press, Inc., New York, 1963), pp. 811-826.

13. Wegener, P. P., "Condensation Phenomena in Nozzles" Heterogeneous Combustion, edited by H. G. Wolfhard, et al. (Academic Press, Inc., New York, 1964), pp. 701-724.

14. Feder, J., et al., "Homogeneous Nucleation in Condensation," Heterogeneous Combustion (Academic Press, Inc., New York, 1964), pp. 667-675.

15. Andres, R. P. and Boudart, M., "Time lag in multistage kinetics," J. Chem. Phys. 42 (6), 2057-2064 (March 1965).

16. Hill, P. G., "Homogeneous nucleation of supersaturated water vapor in nozzles," MIT Gas Turbine Lab. Report No. 78 (January 1965).

17. Stodola, A. and Lowenstein, L. C., Steam and Gas Turbines, (McGraw-Hill, Inc., New York, 1945), 2nd printing, p. 312.

18. Benjamin, M. W. and Miller, J. G., "Flow of water through throttling orifices," Trans. ASME, 419-429 (July 1941).

19. Bailey, J., "Metastable flow of saturated water," Trans. ASME 73 (8), 1109-1116 (November 1951).

20. Wegener, P. P. and Fouring, A. A., "Experiments on condensation of water vapor by homogeneous nucleation in nozzles," Phys. Fluids 7 (3), 352-361 (March 1964).

21. Allard, E. F. and Kassner, J. L., "New cloud-chamber method for the determination of homogeneous nucleation rates, "J. Chem. Phys. 42 (4), 1401-1405 (February 1965).

22. Smigielski, J., "Monodimensional adiabatic flow of a two-phase medium, AGSC Wright Field Report FTD-TT-63-378 (1963).

23. Kliegel, R., "Gas Particle Nozzle Flows," Ninth Symposium on Combustion (Academic Press, Inc., New York, 1963), pp. 811-826.

24. Lowi, A., "Spacecraft jet reaction control," Aerospace Corp., TOR-469(5560-10)-2 (July 1962).

25. Kubin, R. F. and Presley, L. L., "Thermodynamic properties and Mollier chart for hydrogen for 300° to 20,000° K, NASA Ames Research Center, SP-3002 (1964).

26. Dean, J. W., "A tabulation of the thermodynamics properties of normal hydrogen from low temperatures to 540°R and from 10 to 1500 psia," NBS Tech. Note 120 A (June 1962).

27. Din, F., Thermodynamic Functions of Gases (Butterworths, Ltd., London, England, 1961) Vol. 3.

28. "Thermodynamic properties of Freon-14," E. I. DuPont Co., Bulletin T-14 (1961).

29. Griep, D. J., "Electronics program: satellite attitude control system experiments," Aerospace Corp. TDR-269(4250-32)-2 (15 May 1964).

UNCLASSIFIED
Security Classification

DOCUMENT CONTROL DATA - R&D
(Security classification of title, body of abstract and indexing annotation must be entered when the overall report is classified)

1 ORIGINATING ACTIVITY *(Corporate author)*
Aerospace Corporation
El Segundo, California

2a. REPORT SECURITY CLASSIFICATION
Unclassified

2b GROUP

3 REPORT TITLE
DYNAMIC PERFORMANCE OF LOW THRUST COLD GAS REACTION JETS IN A VACUUM

4 DESCRIPTIVE NOTES *(Type of report and inclusive dates)*

5 AUTHOR(S) *(Last name, first name, initial)*
Greer, Harold and Griep, David J.

6 REPORT DATE
August 1966

7a. TOTAL NO. OF PAGES
52

7b. NO. OF REFS
29

8a. CONTRACT OR GRANT NO.
AF 04(695)-669

b. PROJECT NO.

c

d.

9a. ORIGINATOR'S REPORT NUMBER(S)
TR-669(6230-33)-1

9b. OTHER REPORT NO(S) *(Any other numbers that may be assigned this report)*
SSD-TR-66-160

10 AVAILABILITY/LIMITATION NOTICES
This document is subject to special export controls and each transmittal to foreign governments or foreign nationals may be made only with prior approval of SSD (SSTRT).

11. SUPPLEMENTARY NOTES

12. SPONSORING MILITARY ACTIVITY
Space Systems Division
Air Force Systems Command
Los Angeles, California

13 ABSTRACT

The pulsed propulsive performance of low-thrust reaction jets, typical of those used for small spacecraft attitude control, is analyzed and compared with the results of laboratory experiments. Five gases, hydrogen, nitrogen, ammonia, Freon-12, and Freon-14, are investigated using a 48 to 1 expansion ratio nozzle. The transient processes which dominate the short-pulse or limit-cycle mode of thruster operation are formulated. These relationships show good correlation with the data. The apparatus, procedures, and techniques required to obtain accurate test results for a low-thrust, dynamic mode of operation are described. Impulse bit size, gas consumption, and specific impulse are characterized in terms of thruster geometry, gas properties, and command pulse width to provide a basis for optimum system design. A simplified method for calculating dynamic impulse bit size, dynamic gas consumption, and pulsed specific impulse as a function of command pulse width is developed. Finally, the effective performance of the gases tested is evaluated by a technique which includes the influence of tank and propellant weights, as well as specific impulse.

DD FORM 1473 (FACSIMILE)

UNCLASSIFIED
Security Classification

14. KEY WORDS

Low Thrust Propulsion
Reaction Jets
Performance of Reaction Jets
Dynamics of Low Thrust Jets
Transient Performance of Reaction Jets
Attitude Control Propulsion
Transient Impulse Analysis
Cold Gas Propulsive Performance
Specific Impulse of Various Gases
Cold Gas Propulsion
Gas Dynamics of Attitude Control Motors
Pulsed Performance of Reaction Jets
Pulsed Attitude Control Propulsion
Inert Gas Reaction Jets
Spacecraft Vernier Motor Performance
Small Pulse Width Performance
Measurement of Low Thrust Dynamics

Abstract (Continued)

SUPPLEMENTARY

INFORMATION

AD-802 424

AEROSPACE CORPORATION

DOCUMENT CHANGE NOTICE

TO: Copyholders

CC:

DATE: 6 April 1967

SUBJECT: Removal of Distribution Limitation on TR-669(6230-33)-1

FROM: Publications Section
Reports Control Group

Please make the following pen and ink changes to subject report, entitled "Dynamic Performance of Low Thrust Cold Gas Reaction Jets in a Vacuum," by H. Greer and D. J. Griep:

1. In the Foreword, please strike out the entire paragraph beginning with "Information in this document is embargoed. . ."

2. Strike out and replace the distribution statement on the title page and DD Form 1473 with the following:

DISTRIBUTION OF THIS DOCUMENT IS UNLIMITED

This action is authorized by the DOD controlling agency, Space Systems Division (SSTP).